http://app.pan.pl/SOM/app66-Braunn_etal_SOM.pdf

SUPPLEMENTARY ONLINE MATERIAL FOR

Enamel microstructure of permanent and deciduous teeth of notoungulate *Toxodon*: Development, functional, and evolutionary implications

Patrícia R. Braunn, Jorge Ferigolo, and Ana M. Ribeiro

Published in *Acta Palaeontologica Polonica* 2021 66 (2): 449-464.
https://doi.org/10.4202/app.00772.2020

Supplementary Online Material

SOM 1. Fig. 1. Dental morphology and terminology in transversal cross-section showing occlusal view of permanent (A–C) and deciduous cheek teeth (D–E) of *Toxodon* sp.

SOM 2. Table 1. Data about enamel microstructure of 26 histological sections obtained from 13 specimens of *Toxodon* sp. belonging to Museu Coronel Tancredo Fernandes de Mello (Santa Vitória do Palmar), Museu de Ciências Naturais (Porto Alegre) and Museu Nacional (Rio de Janeiro) paleontological collections examined.

SOM 3. Enamel microstructure of *Toxodon* sp. from southern Coastal Plain of Rio Grande do Sul State, Brazil; Santa Vitória Formation (Late Pleistocene).

Fig. 1. I1 (MCN-PV 9907; MCN-PHIS 053)
Fig. 2. I2 (MCN-PV 1162; MCN-PHIS 054)
Fig. 3. i1 (MN 2372-C)
Fig. 4. i3 (MCN-PV 9879; MCN-PHIS 056)
Fig. 5. M3 (MCN-PV 30077; MCN-PHIS 55).
Fig. 6. Lower molariform teeth. A–C, p4, MCN-PV 9731 [MCN-PHIS 57]; D–F, m1– 2, MCN-PV 9902 [MCN-PHIS 52].
Fig. 7. m1–2 (MCN-PV 9902; MCN-PHIS 52)
Fig. 8. m1–2 (MCN-PV 9902; MCN-PHIS 52)
Fig. 9. dP4 (MCN-PV 36937). A, C, [MCN-PHIS 44]; B. [MCN-PHIS 46]
Fig. 10. dP4 (MN 2372A and MN 2372B). A, (MCN-PHIS 24); B, C, (MCN-PHIS 17); D, (MCN-PHIS 25); E, (MCN-PHIS 26).
Fig. 11. dp4 (MCTFM-PV 0793) A, B; [MCN-PHIS 30]; C, D. [MCN-PHIS 50].

SOM 1. Fig. 1. Dental morphology and terminology in transversal cross-section showing occlusal view of permanent (A–C) and deciduous cheek teeth (D–E) of *Toxodon* sp. A, upper molar (right M2); B, lower molar (left m3); C, lower premolar (right p4); D, upper premolar (right dP4); E, lower premolar (left dp4). The darker lines indicate where enamel occurs. Not to scale. Dental nomenclature follows Madden (1997).

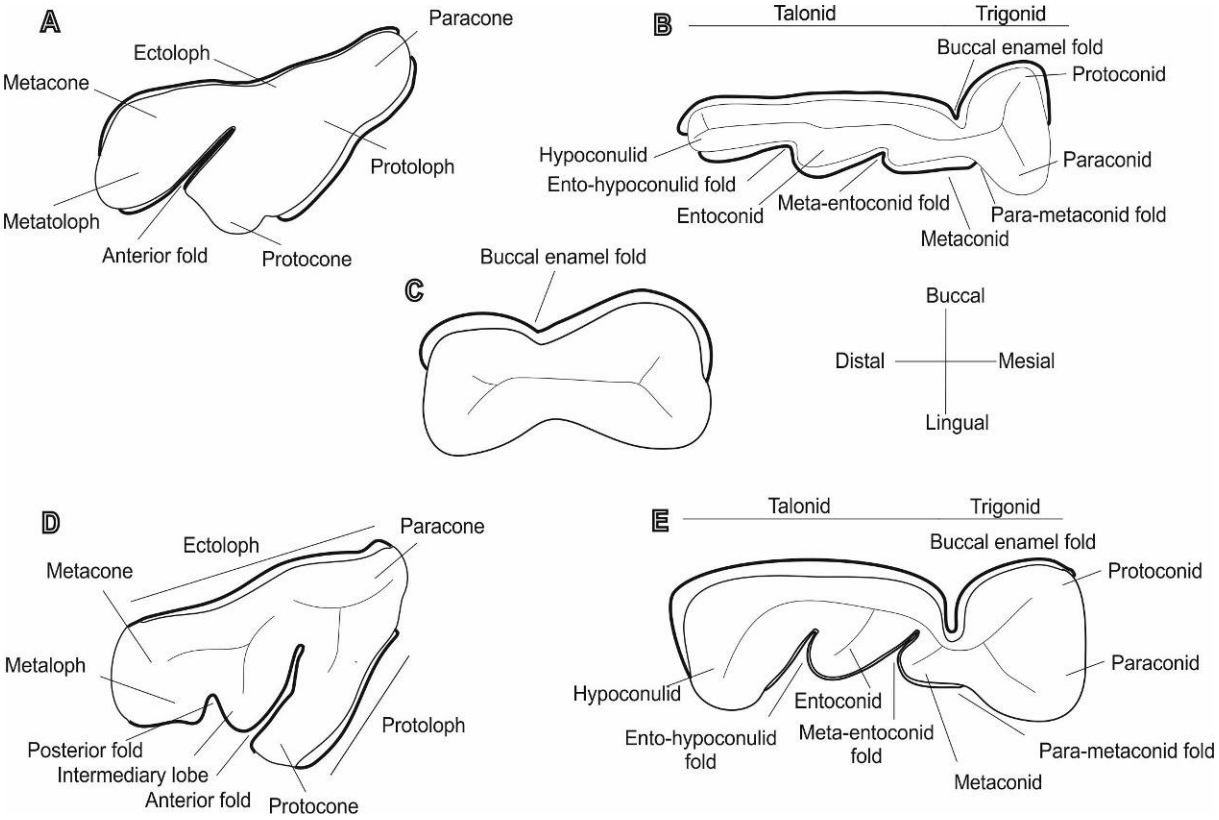

SOM 2. Table 1. Data about enamel microstructure of 26 histological sections obtained from 13 specimens of *Toxodon* sp. belonging to Museu Coronel Tancredo Fernandes de Mello (Santa Vitória do Palmar), Museu de Ciências Naturais (Porto Alegre) and Museu Nacional (Rio de Janeiro) paleontological collections examined. ** could not be viewed. MRE, modified radial enamel; HSB, Hunter-Schreger bands; RE, radial enamel; HSBi (deg), angle of inclination of the HSB.

Specimen number	Tooth	Number histological collection	Orientation of sectioning plane	Buccal/lingual	Crown portion	Enamel thickness (µm)	MRE %	HSB %	RE %	HSB_i (deg)	Prisms per HSB
UPPER TEETH											
MCN-PV 9907	I1	MCN-PHIS 53	longitudinal	buccal	-	970-1000	18	60	22	60-70	6-9
MCN-PV 1162	I2	MCN-PHIS 54	longitudinal	buccal	apical	1.170-1.320	**			-	-
					lateral	1.050-1.070	10	53	37	45-65	9-16
MCN-PV 36937	dP4	MCN-PHIS 44	longitudinal	buccal	ectoloph (distal)	480-610	33	48	19	45-55	9-12
			longitudinal	lingual	metacone (distal)	680-840	**				
		MCN-PHIS 46	transversal	buccal	ectoloph (distal)	520-650	**				
				lingual	metacone (distal)	330-440	-	-	100	-	-
				lingual	protocone (anterior fold)	210-720	-	-	100	-	-
MN 2372-A	dP4	MCN-PHIS 17	transversal	lingual	protocone	77-130	26	53	21	-	-
MN 2372-B	dP4	MCN-PHIS 24	longitudinal	lingual	protoloph (mesial)	610-840	17	83	-	45-55	6-10
		MCN-PHIS 25	transversal	lingual	anterior fold (distal)	200-400	-	-	100	-	-
				lingual	protoloph (mesial-distal)	460-760	**				
				buccal	ectoloph (mesial-distal)	450-630	**				
		MCN-PHIS 26	transversal	lingual	anterior fold (distal)	150-300	-	-	100	-	-
				lingual	protoloph (mesial-distal)	300-580	**				
				buccal	ectoloph (mesial-distal)	360-520	**				
MCN-PV 30077	M3	MCN-PHIS 55	transversal	buccal	ectoloph (mesial-distal)	1.000	24	56	20	45-50	7-12
				lingual	anterior fold (distal)	390-810	20	80	-	45	6-13
LOWER TEETH											
MN 2372-C	i1	MCN-PHIS 01	longitudinal	buccal	mesial	1.250-1.420	15	55	30	70	15-20
		MCN-PHIS 08	longitudinal	buccal	mesial	1.120	-	-	-	-	-
		MCN-PHIS 09	longitudinal	buccal	distal	670	32	36	32	45-60	8-10
		MCN-PHIS 03	transversal	buccal	distal	620-960	22	50	28	-	-
		MCN-PHIS 04	transversal	buccal	distal	850-1000	16	58	26	-	-
		MCN-PHIS 05	transversal	buccal	distal	680-990	16	66	18	-	-
		MCN-PHIS 06	transversal	buccal	distal	990	17	53	30	55-75	7-12
MN 2938-V	i?	MCN-PHIS 20	transversal	buccal	-	1.000	12	50	38	45-55	-
		MCN-PHIS 22	transversal	buccal	-	920-1.340	26	66	8	-	-
		MCN-PHIS 23	transversal	buccal	-	420-1.100	14	52	34	30-40	7-10
MCN-PV 9879	i3	MCN-PHIS 56	transversal	buccal	-	720-890	12	56	32	45-55	10
MCN-PV 9731	p4	MCN-PHIS 57	transversal	buccal	along buccal enamel	1.200-1280	7	53	40	40-50	15-20
MCN-PV 9738	p4	MCN-PHIS 58	transversal	buccal	buccal enamel fold	430-960	**				

MCTFM-PV 0793		MCN-PHIS 30	longitudinal	buccal	paraconid	760-990	7	47	46	45-60	5-10
				lingual	protoconid	960-1.410	-	-	100	-	-
		MCN-PHIS 33	transversal	buccal	talonid	790-960	-	-	100	-	-
				buccal	trigonid	480-920	**				
				buccal	buccal enamel fold	300	**				
				lingual	paraconid	550-610	-	-	100	-	-
				lingual	metaconid	450-670	-	-	100	-	-
				lingual	meta-entoconid fold	290-450	-	-	100	-	-
		MCN-PHIS 50	transversal	buccal	paraconid	420-950	-	-	100	-	-
				mesial	paraconid	280-500	-	-	100	-	-
				lingual	metaconid	610-730	-	-	100	-	-
MCN-PV 9902	m1–2?	MCN-PHIS 52	tangencial	buccal	talonid	640-1.760	**				
				buccal (distal)	hypoconulid	1.150-1.380	10	60	30	60-65	5-6
				lingual	ento-hypoconulid fold (internal)	840-1.120	**			-	-
					ento-hypoconulid fold (mesial loop)	210-830	32	51	17	45-50	14-18
					ento-hypoconulid fold (distal loop)	830-950	23	50	27	60-65	4-12
					metaconid	740-1.340	**			-	-
					meta-entoconid fold (internal)	500-900	22	63	15	-	6-20
					meta-entoconid fold (mesial close to internal loop)	540-680	44	56	-	50	**
					meta-entoconid fold (mesial loop)	600-740	33	45	22	25-50	**
					meta-entoconid fold (distal loop close to internal loop)	780-820	14	49	37	60-70	10-20
					meta-entoconid fold (distal loop)	890-1.230	43	38	19	75-90	10-20
		MCN-PHIS 59	transversal	buccal	hypoconulid	930-1020	21	49	30	-	-
				lingual	entoconid	880-950	10	66	24	-	-

SOM 3. Fig. 1. Enamel microstructure in I1 (MCN-PV 9907.PHIS-053) of *Toxodon* sp. from southern Coastal Plain of Rio Grande do Sul State, Brazil; Santa Vitória Formation (Late Pleistocene). Scanning electron micrographs of longitudinal sections through the dental axis; A, Schmelzmuster exhibiting three enamel types: MRE (below the inferior dashed line); HSB (between dashed lines); and RE in the outer enamel surface; B, general view of intermediary and external zone of enamel. HSB show alternate thick and thin vertical zones with distinct heights; C, detail of the HSB observed in B.

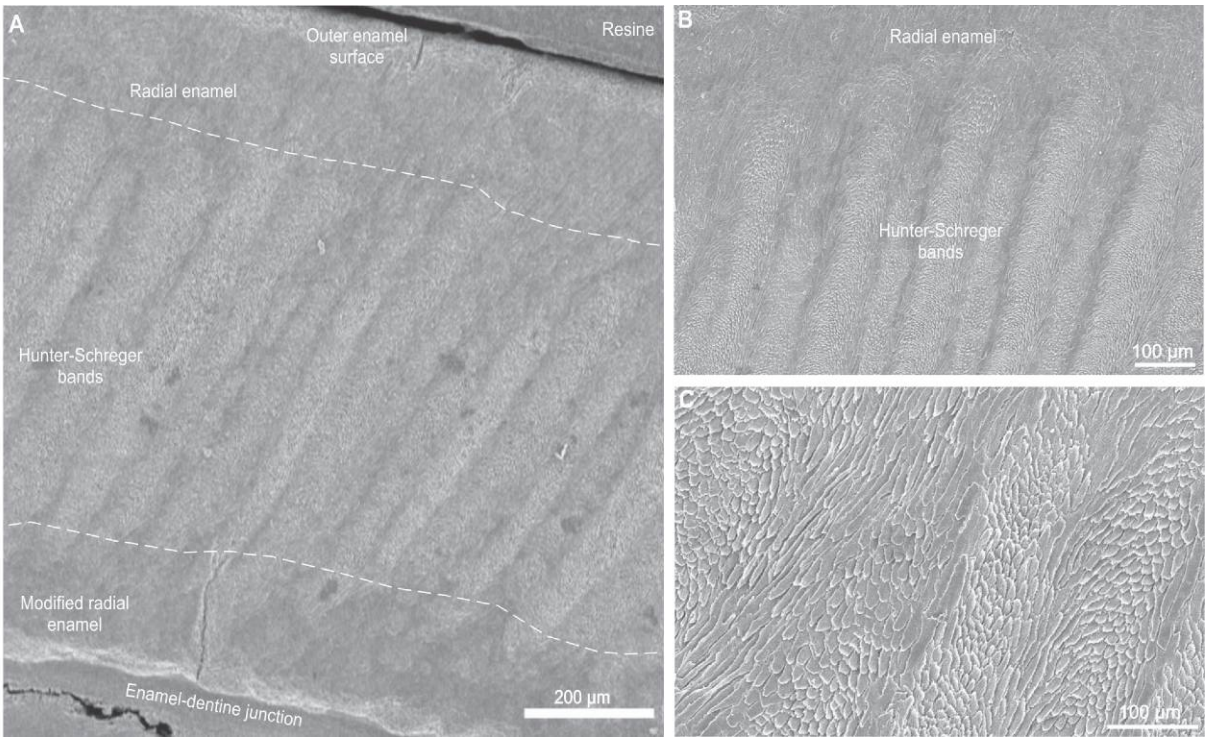

SOM 3. Fig. 2. Enamel microstructure in I2 (MCN-PV 1162.PHIS-054) of *Toxodon* sp. from southern Coastal Plain of Rio Grande do Sul State, Brazil; Santa Vitória Formation (Late Pleistocene). Scanning electron micrographs of longitudinal sections through the uppermost and labial side of the dental axis; A, detail of HSB; B, prisms close to the OES; C, prisms of RE; D, MRE. White arrows indicate two regularly spaced striae of Retzius; black arrow shows a fissure between enamel prisms. Scalloped EDJ (dashed line).

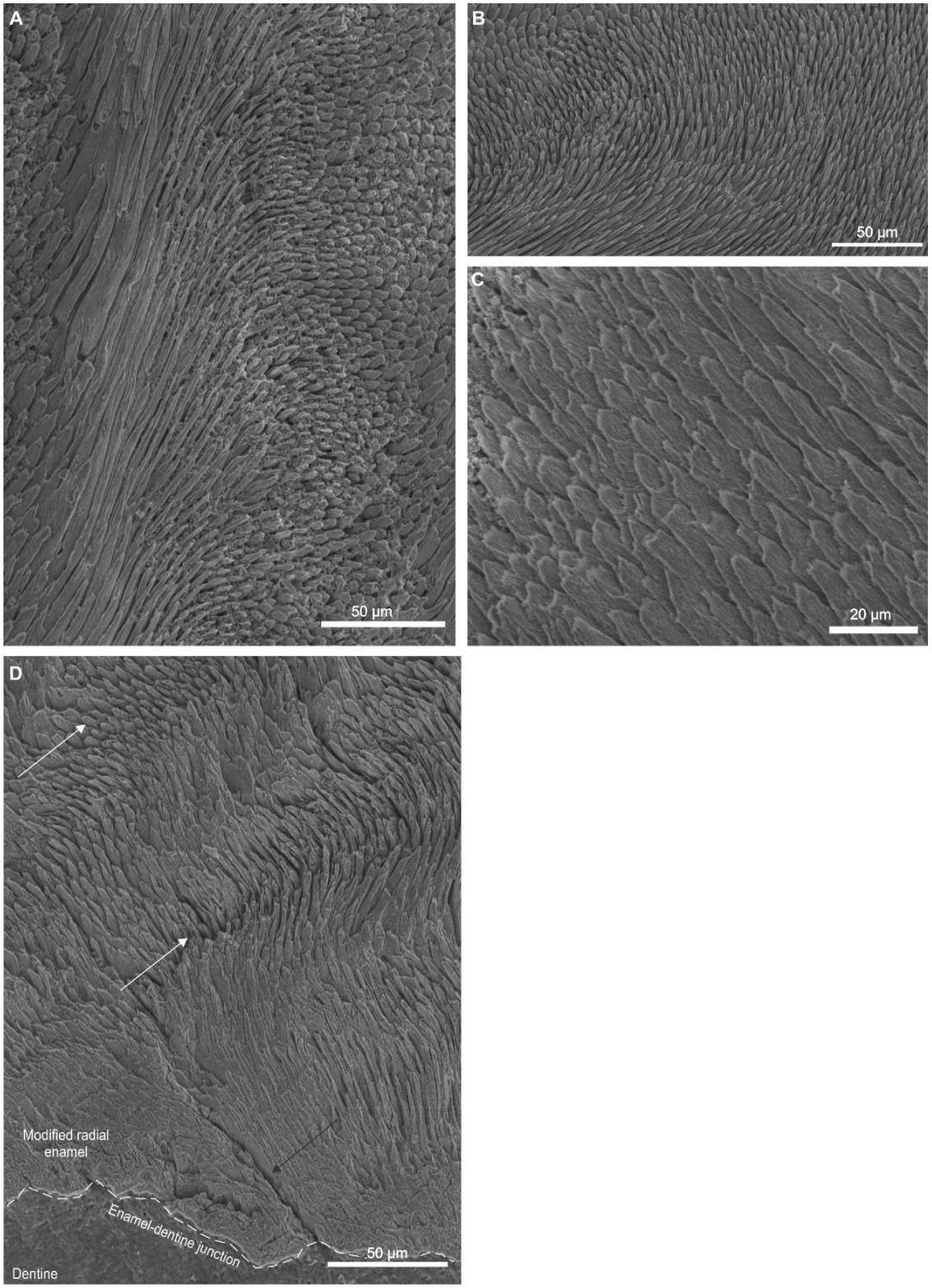

SOM 3. Fig. 3. Enamel microstructure of i1 (MN 2372-V.C) of *Toxodon* sp. from São Paulo State, Brazil (Late Pleistocene). Scanning electron micrographs of longitudinal (A–C, E, F), tangential (D) and transversal (F) sections of the buccal side in the lowermost mesial (A–C) and distal (C, E–F) portions of the dental axis; A–B, [MCN-PHIS 008]; A, HSB; B, detail of transitional zones (arrows) between HSB; C, E–F [MCN-PHIS 009]; C, general view of enamel exhibiting Schmelzmuster with three enamel types. Note enamel incremental lines close to the OES (dotted lines); D, [MCN-PHIS 001] transitional zones (arrows) between HSB. Note MRE (below the dashed line) showing IPM parallel to the prisms; E, partial view of enamel showing MRE and HSB. Smooth EDJ (dotted line); F, prisms of RE.

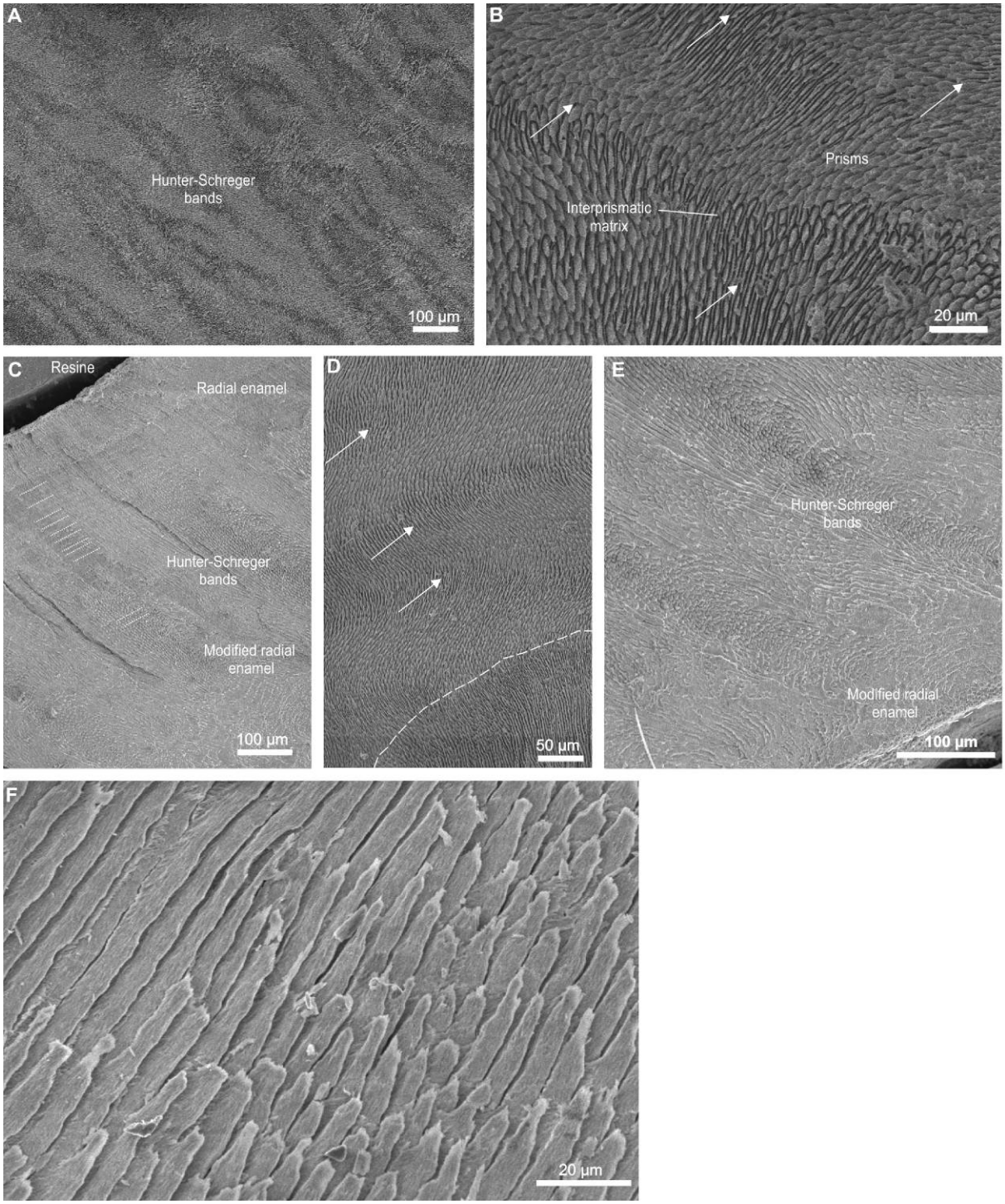

SOM 3. Fig. 4. Enamel microstructure of i3 (MCN-PV 9879.PHIS-056) of *Toxodon* sp. from southern Coastal Plain of Rio Grande do Sul State, Brazil; Santa Vitória Formation (Late Pleistocene). Scanning electron micrographs of transversal section of the uppermost portion through the dental axis. A, HSB. Note the change of prism direction between the vertical bands, where it is possible to observe the plates of IPM parallel to the prisms (arrows); B, HSB bent on their way to the OES; C, prisms close to the OES.

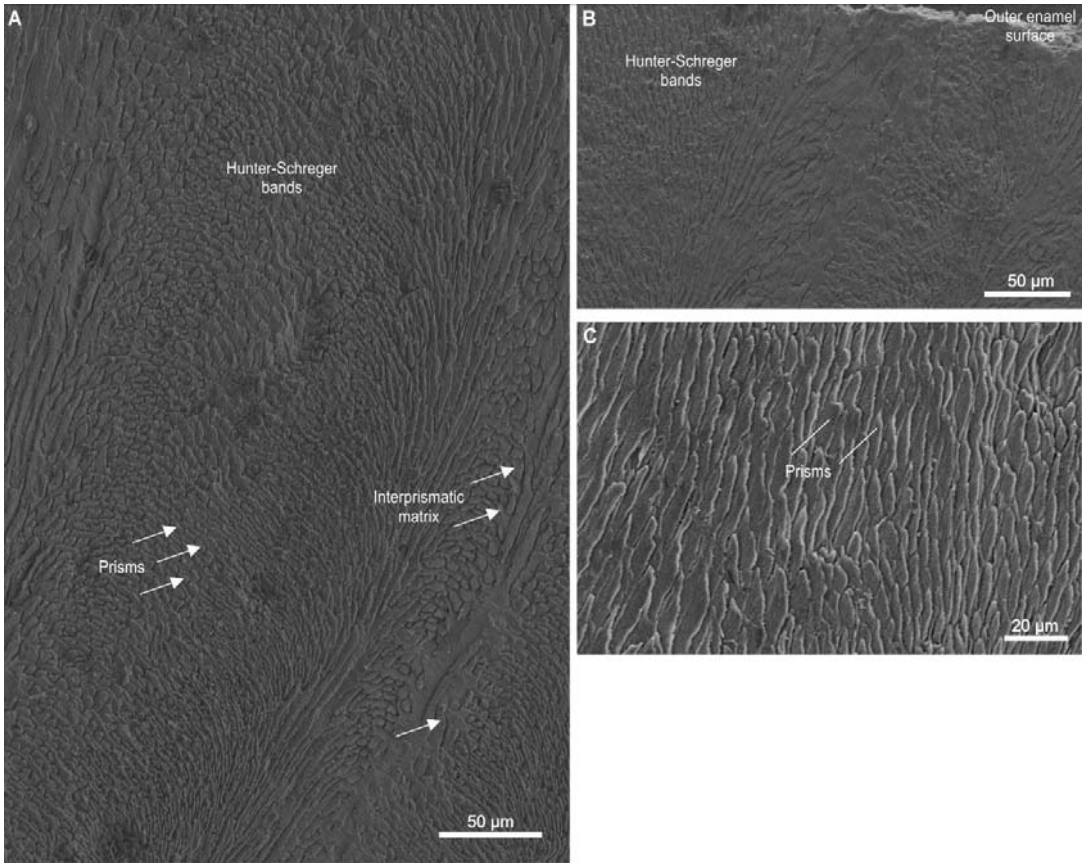

SOM 3. Fig. 5. Enamel microstructure in M3 (MCN-PV 30077.PHIS 55) of *Toxodon* sp. from southern Coastal Plain of Rio Grande do Sul State Brazil; Santa Vitória Formation (Late Pleistocene). Scanning electron micrographs of transversal sections of the ectoloph. A, detail of HSB. Note the change of prism direction between the vertical bands, where it is possible to observe the plates of IPM parallel to the prisms (white arrows); B, prisms of RE.

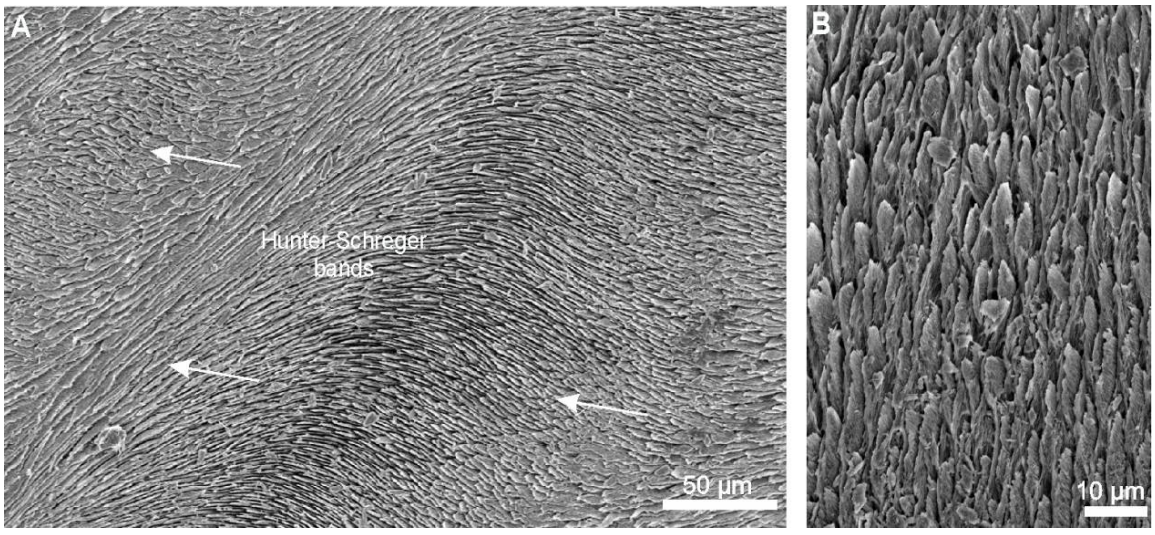

SOM 3. Fig. 6. Enamel microstructure in lower molariform teeth of *Toxodon* sp. from southern Coastal Plain of Rio Grande do Sul State, Brazil; Santa Vitória Formation (Late Pleistocene). Scanning electron micrographs of transversal section of the buccal side of the lowermost portion through the dental axis (A–C), and tangential section through mesial side of the uppermost portion through the dental axis (D–F). A–C, p4, MCN-PV 9731.PHIS-57; A, HSB; B, prisms of RE; C, MRE close to the EDJ (dashed line); D–F, m1–2, MCN-PV 9902.PHIS-52; D, prisms of RE; E, HSB and MRE close to the EDJ (dashed line); F, detail of HSB observed in E, exhibiting thick and thin alternate vertical bands.

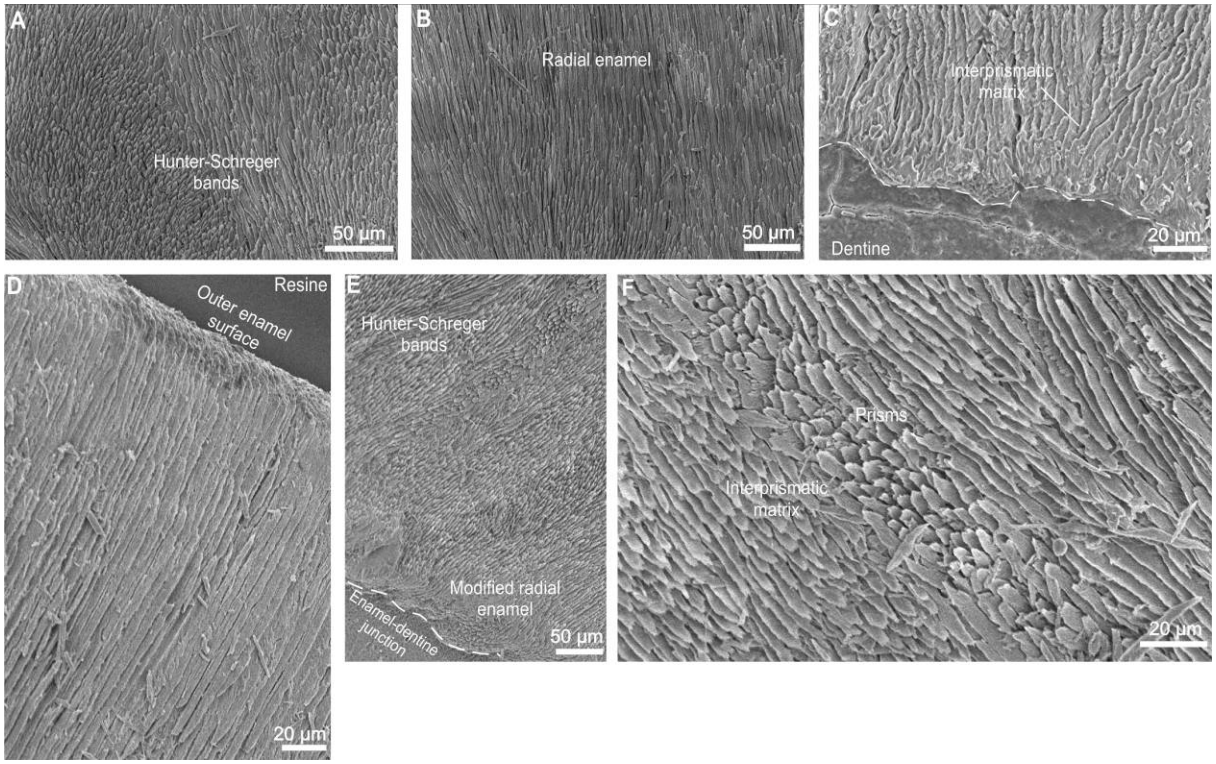

SOM 3. Fig. 7. Enamel microstructure in m1–2 (MCN-PV 9902.PHIS-52) of *Toxodon* sp. from southern Coastal Plain of Rio Grande do Sul State, Brazil; Santa Vitória Formation (Late Pleistocene). Scanning electron micrographs of tangential section of the lingual side of the uppermost portion through the dental axis. A, undulating pattern of HSB, parallel to the EDJ (dashed line); B, detail of HSB observed in A.

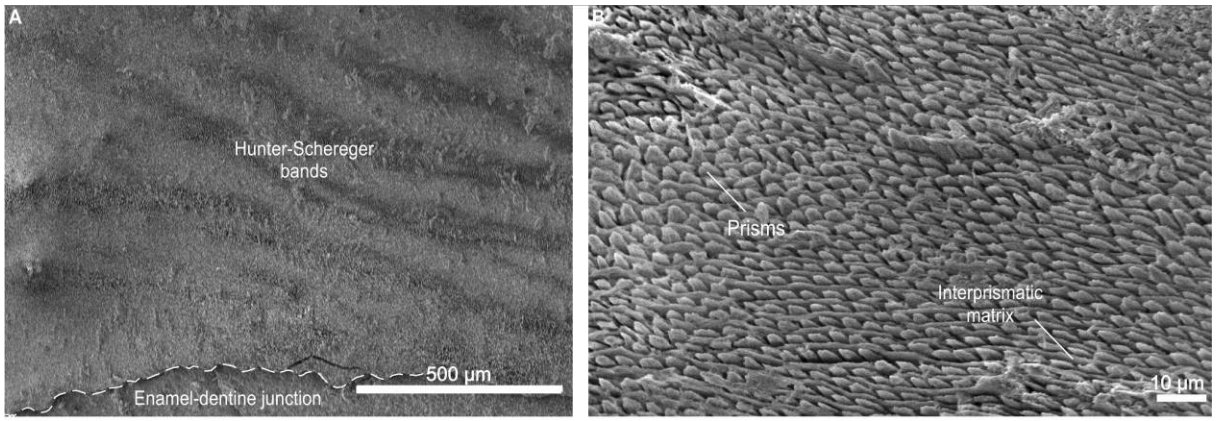

SOM 3. Fig. 8. Enamel microstructure in m1–2 (MCN-PV 9902.PHIS-52) of *Toxodon* sp. from southern Coastal Plain of Rio Grande do Sul State, Brazil; Santa Vitória Formation (Late Pleistocene). Scanning electron micrographs of tangential section through the lingual side of the uppermost portion of the dental axis. A, detail from decussation of prisms under the hypoplastic defect; B, HSB and MRE close to scalloped EDJ (dashed line); C, detail of MRE with enlarged empty space; D–E, enamel types. Note MRE with large plates of IPM (arrows); F, detail of prisms in the RE observed in D and E.

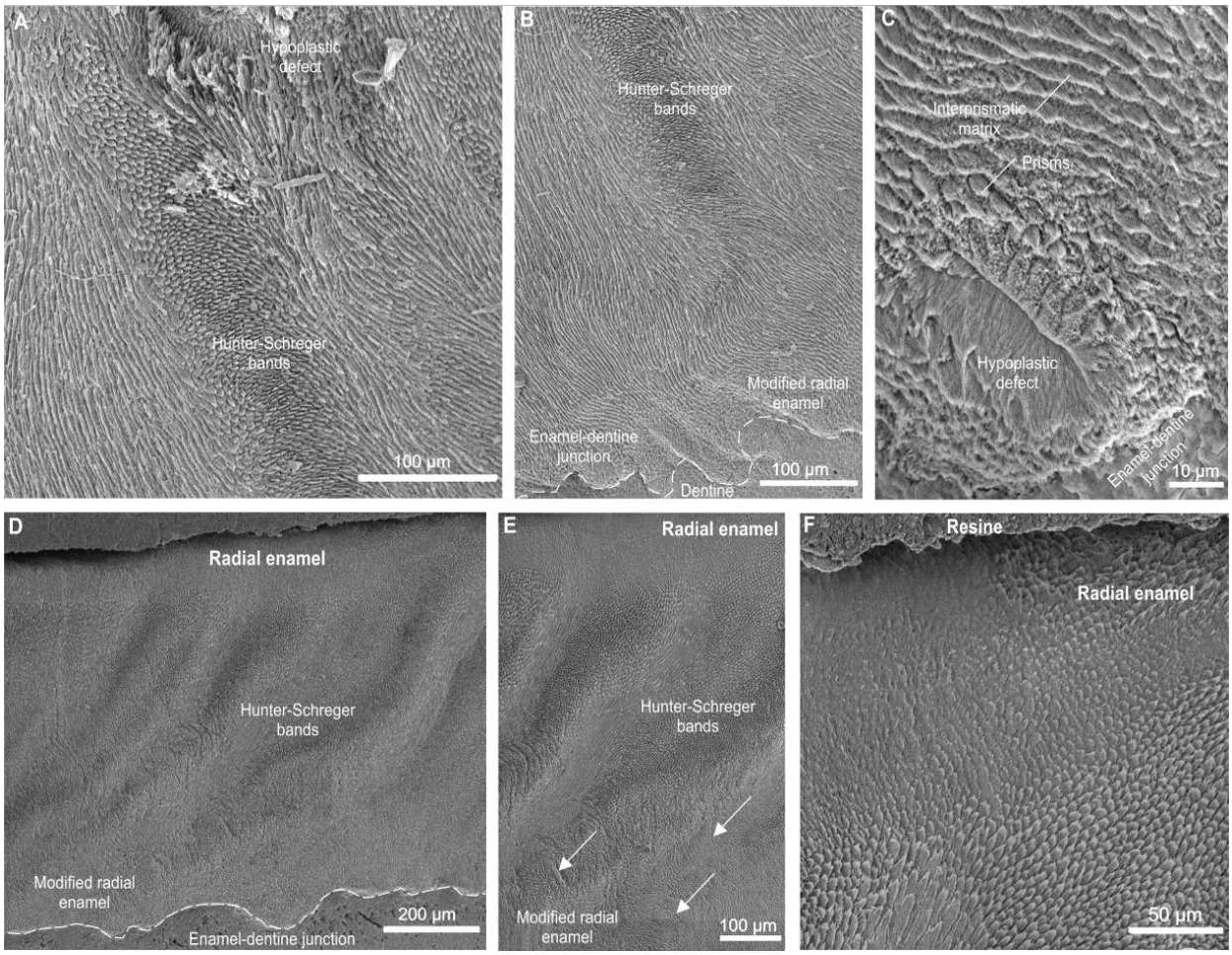

SOM 3. Fig. 9. Enamel microstructure in dP4 (MCN-PV 36937) of *Toxodon* sp. from southern Coastal Plain of Rio Grande do Sul State, Brazil; Santa Vitória Formation (Late Pleistocene). Scanning electron micrographs of longitudinal (A, C) [MCN-PHIS 44] and transversal (B) [MCN-PHIS 46] sections of the lowermost portion through the dental axis; A, detail of intersection of prisms and IPM in MRE; B, distal loop of anterior fold on the metaloph. It is not possible to observe prisms between the thick plates of IPM. C, detail of RE. Note the decussation between the prisms and IPM of HSB under the RE (white arrows).

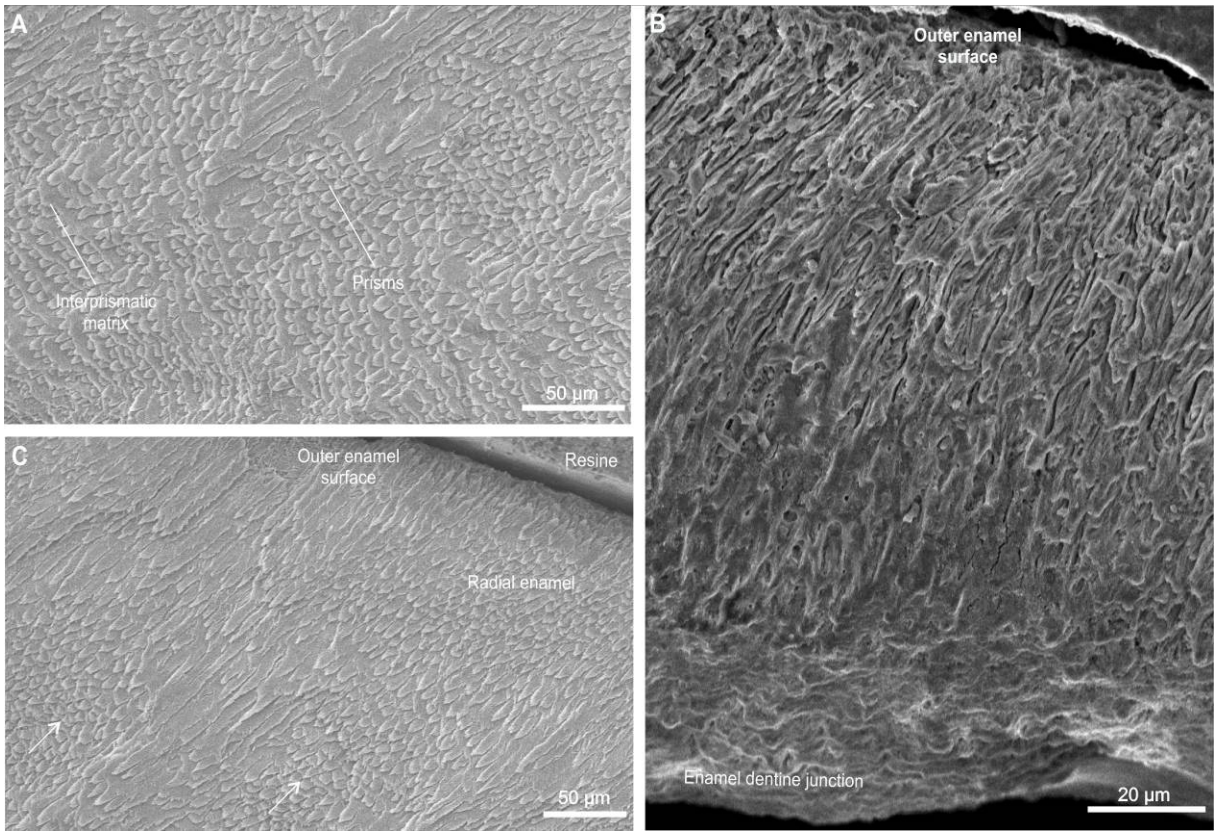

SOM 3. Fig. 10. Enamel microstructure in dP4 (MN 2372-V.A and MN 2372-V.B) of *Toxodon* sp. from São Paulo State, Brazil (Late Pleistocene). Scanning electron micrographs of longitudinal (A) and transversal (B–E) sections of the lowermost portion through the dental axis; A (MCN-PHIS 24); MRE; B–C (MCN-PHIS 17); B, lingual enamel on the protocone with a hypoplastic defect. Under the defect it is possible to observe three enamel types. Note a vascular channel in the area of dentine under the defect (black arrow); C, higher magnification of HSB observed in C; D (MCN-PHIS 25) lingual enamel on the innermost loop of anterior fold; E (MCN-PHIS 26); RE exhibiting prisms parallel to the IPM.

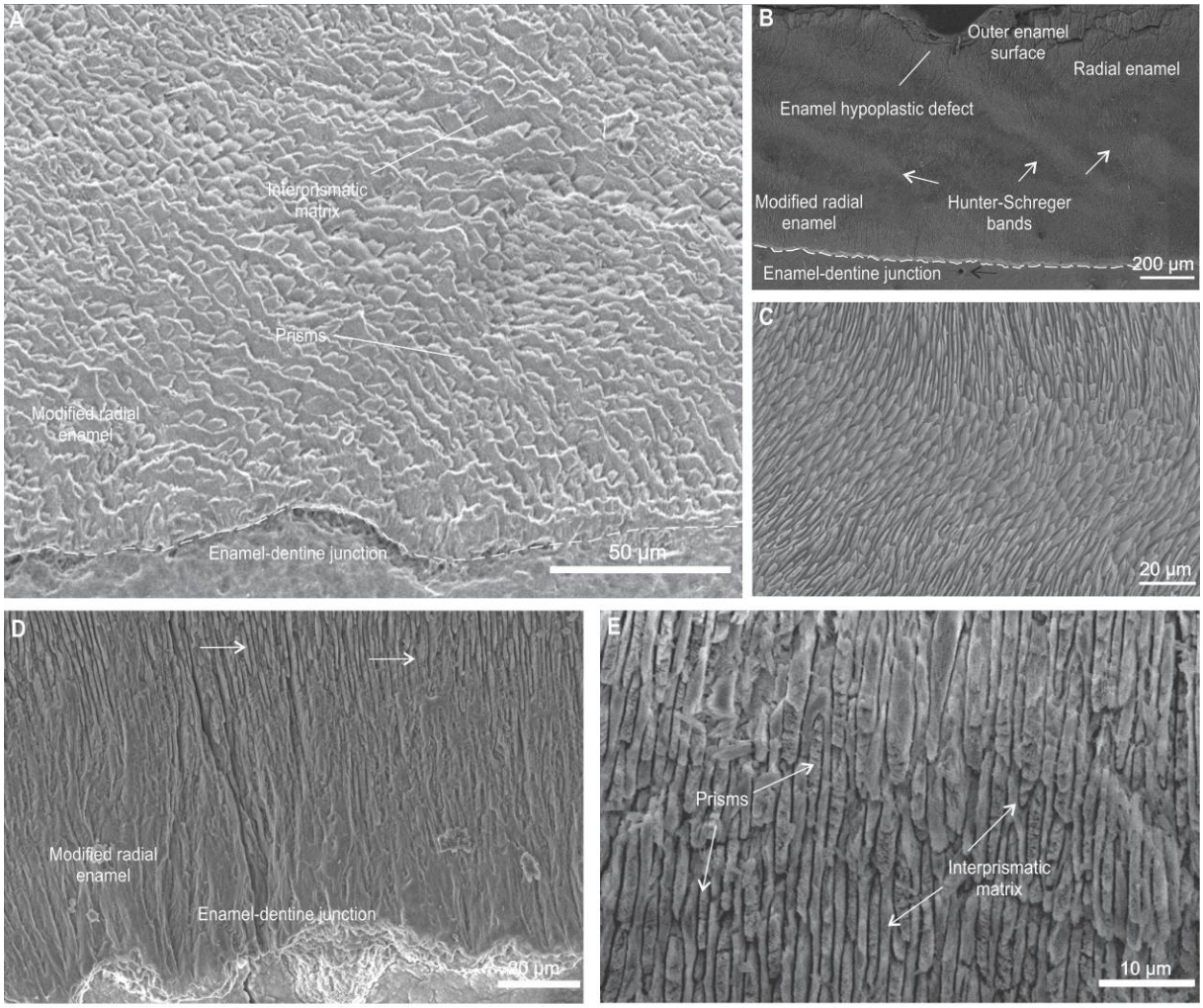

Fig. 11. Enamel microstructure in dp4 (MCTFM-PV 0793) of *Toxodon* sp. from southern Coastal Plain of Rio Grande do Sul State, Brazil; Santa Vitória Formation (Late Pleistocene). Scanning electron micrographs of longitudinal sections of the uppermost portion through the trigonid (A–B) [MCN-PHIS 30] and transversal sections through the trigonid and paraconid (C–D) [MCN-PHIS 50]; A, HSB; B, portion of enamel next to the EDJ with wide plates of IPM surrounding the prisms and the intermediary layer with the HSB; C, parallel distribution between prisms and IPM; D, portion of buccal enamel fold showing parallel distribution between prisms and IPM. Dashed lines indicate scalloped EDJ (B–D).